Liquid Crystals
Publication details, including instructions for authors and subscription information:
http://www.informaworld.com/smpp/title~content=t713926090

Optical birefringence and dichroism in physical steroid organogels

P. Terech[a]
[a] Institut Laüe Langevin, Grenoble Cedex, France

To cite this Article Terech, P.(1991) 'Optical birefringence and dichroism in physical steroid organogels', Liquid Crystals, 9: 1, 59 — 70
To link to this Article: DOI: 10.1080/02678299108036765
URL: http://dx.doi.org/10.1080/02678299108036765

LIQUID CRYSTALS, 1991, VOL. 9, NO. 1, 59–70

Optical birefringence and dichroism in physical steroid organogels

by P. TERECH
Institut Laüe Langevin, 156X, 38042 Grenoble Cedex, France

(*Received 25 April 1990; accepted 5 August 1990*)

Optical birefringence and dichroism have been studied in physical steroid organogels. We have used two complementary derivatives (SNH and SNO*) in cyclohexane: the former has no chromophoric group in the 220–800 nm wavelength range studied, in contrast with the latter. The dichroism is mainly due to linear contributions. The amplitude of the signal is correlated with the growth of fibrillar structures and specially with the heterogeneities of the gel network which was assumed to be chiral fibrillar junction zones. The characteristic SNO* dichroic absorptions (for $C \approx 2{\cdot}0 \times 10^{-2}$ M) are $\lambda_{max} = 250$ nm, $|\Delta\varepsilon| \approx 6{\cdot}0$ (mainly a linear contribution) and $\lambda_{max} = 450$ nm, $\Delta\varepsilon = +0{\cdot}45$ (mainly a circular contribution). These preliminary observations provide strong evidence for a helical stacking of the steroid molecules within the fibres of the gel samples. The optical dichroic absorption can be a valuable technique to monitor the orientational order of the microdomains crossed by the light beam.

1. Introduction

A class of steroid compounds [1, 2] derived from cholesterol, is known to give thermoreversible gel phases in apolar organic solvents. The structure of the porous gel network has been studied extensively mainly by electron microscopy [3] and small angle neutron scattering techniques [4]. The molecular organization and thermodynamic stability are solvent-dependent [5]. The network is constituted of very long fibres, the overall diameter of which is *c.* 9·5 nm; the fibre is formed by mixing two or more finer fibrils. The rod-like steroid aggregates can be locally oriented in microdomains exhibiting the birefringence of schlieren optical textures [5] typical of nematic-like lyotropic phases. Orientation effects can be obtained by varying the following experimental parameters: the steroid concentration (nematic–isotropic transition by excluded volume effects for rod-like objects [5]), the solvent type (influence upon the rigidity of the steroid fibre [4]), or by use of external forces (a strong magnetic field applied during the sol–gel transition [6]).

The steroid molecule is optically active due to the seven asymmetric carbons of its skeleton. The steroid aggregation proceeds via a multiple hydrogen bonding step which connects the individual molecules within the rod-like fibre. Considering the chirality of the individual steroid molecules, it is expected that the aggregate exhibits chirality in some level of its molecular or supramolecular organization. This is already evidenced by electron micrographs obtained form a special freeze–etching procedure [3] which we have adapted for the case of apolar solvents: helicity is encountered at a primary level in the constitutive fibrils of the steroid fibre (pitch $< 10{\cdot}0$ nm) and at a larger scale as twists in the superstructure of the fibres (corresponding to a pitch of several tens of nanometers).

We want to study here by a non-perturbing (compared to electron microscopy techniques) and more unequivocal method (compared to the small angle neutron

0267-8292/91 $3.00

scattering technique) the existence of a chiral organization in the steroid gel network. Optical techniques (complex birefringence) are suited to analyse the interferences of light with structures in the range of colloidal distances. The results are discussed on the basis of the few data available in the field of physical gels.

2. Experimental

The synthesis [1] and the preparation [5] of gel samples have been described elsewhere. We consider in the following only the protonated solvent cyclohexane (Gold Label) from Aldrich which was used as received. Gels are obtained either with the paramagnetic nitroxide SNO* compound or with the diamagnetic amine SNH compound (see figure 1). The critical concentration where the sol–gel transition occurs at room temperature is $0{\cdot}8 \times 10^{-2}$ M (SNO*) and $1{\cdot}4 \times 10^{-2}$ M (SNH). A Dichrographe III Jobin–Yvon spectropolarimeter was used in the range 180–800 nm to study the optical dichroism. Hellma quartz cells from 0·001 to 0·1 dm thick were used. The optical rotatory power was measured with a Jobin–Yvon digital micropolarimeter. The apparatus can measure the angular deviation range $-0{\cdot}6/+0{\cdot}6°$ at four wavelengths (436, 546, 578, 589 nm). The birefringence Δn (the difference of the refractive indices of light linearly polarized parallel and perpendicular to a reference direction) was measured using a combined photoelastic modulation and compensation technique [7]. The compensation was made by means of a Pockels cell and the resulting resolution was 10^{-10}; Δn was measured at 632·8 nm. For orientation experiments, the magnetic field was produced by a Brucker NMR spectrometer ($B = 4{\cdot}2$ T: dichroism measurements) or by a water cooled, Bitter-type solenoid ($B = 7$ T: birefringence measurements). All of the experiments are performed at room temperature.

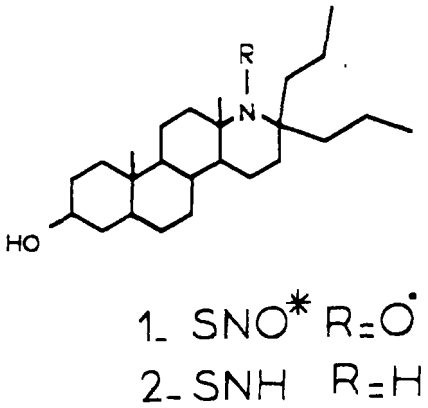

Figure 1. The two gelling steroid derivatives SNH and SNO*. The asterisk denotes the single electron of the nitroxide group.

3. Results

A uniaxial material which is both birefringent and dichroic can be described by the complex birefringence Δn^* [8]

$$\Delta n^* = \Delta n' - i\Delta n'', \tag{1}$$

where the real part $\Delta n'$ is the circular birefringence and $\Delta n''$ is the imaginary part or the circular dichroism. This definition holds for molecules in dilute solutions but for

concentrated solutions or colloidal systems, the physics can be especially complicated. For some macromolecules, for instance an infinite helical polymer, models are available which make use of the classical polarizability theory [9]. $\Delta n'$ and $\Delta n''$ can be conveniently described by considering the resulting action on the two circularly polarized components (L and R indicate left and right, respectively) of linearly polarized light. For an optically active system, the circular birefringence is expressed as

$$\left.\begin{aligned} \alpha &= \frac{1800}{\lambda}(n_L - n_R), \\ [\alpha] &= \frac{\alpha}{dc}, \end{aligned}\right\} \tag{2}$$

where n_L is the refractive index, i.e. the relative velocity of the left handed component, α being the measured optical rotation (degrees), d is the optical path length in decimeters, c is the concentration in $g\,cm^{-3}$ and $[\alpha]$ is the specific rotatory power.

For the imaginary part, when the absorption coefficients K_R, K_L are different, dichroism absorption occurs in a wavelength range when there is an effective light absorption by a chromophoric group. The resulting light becomes elliptically polarized

$$\left.\begin{aligned} I &= I_0 \exp(-Kd) \\ [\theta] &= \frac{\psi M}{100dc} = 3300\Delta\varepsilon. \end{aligned}\right\} \tag{3}$$

Here ψ is in degrees, $[\theta]$ is the molar ellipticity in degree cm^2 $(d\,mol)^{-1}$ and M is the molecular mass of the active solute. The rotational strength of an electronic transition is the scalar product of the electric transition moment and the magnetic transition moment so that weak UV transitions can give significant dichroic absorptions. This is the case for SNO* for which the only chromophoric group is the nitroxide group which is a weak UV absorber.

It is worth noting that selective absorption is not the only phenomenon which can be detected. In given cholesteric systems a dichroic signal is attributed to a selective reflection of light by the helical structure. In these cases, the so-called de Vries equations [10] are used to evaluate the related pitches,

$$\lambda_{max} = nP. \tag{4}$$

Here λ_{max} is the wavelength of maximum reflectivity, n is the average refractive index and P is the pitch.

Frequently the vectorial composition of the electrical dipoles between structured neighbours adds a linear component, the intensity of which may be important. On the one hand concerning birefringence, the linear term is that observed in connection with the typical optical textures of the lyotropic system [5] and measured by the compensation technique. On the other hand, the observed dichroic signal is a superimposition of circular and linear components

$$\left.\begin{aligned} [\theta]_{obs} &= [\theta]_{real} + [\theta]_{LD}, \\ [\theta]_{obs}(\alpha) &= [\theta]_{real} + K[\theta]_{LD}\cos(2\alpha). \end{aligned}\right\} \tag{5}$$

The linear contribution (LD) can be estimated (or eliminated) by averaging the signal intensities taken at all orthogonal angles (α) of the cell in the plane normal to the light

beam [11]. Following from equation (5), $[\theta]$ has a maximal value with opposite signs for orthogonal angles (α and $\alpha + \pi/2$) in a fully oriented system. A rough estimation of the orientational contribution to the observed signal $[\theta]_{obs}$ can be obtained from

$$R_\lambda = \frac{[\theta](\alpha)}{[\theta](\alpha + \pi/2)}. \quad (6)$$

In a fully oriented system $R = -1$, for a pure circular contribution $R = 1$ while for a partially oriented volumic system the highest positive values correspond to the lowest orientation order and lowest negative ones to the best order.

3.1. *Non-gelling dilute solutions*

The present optical measurements for SNO* and SNH solutions in cyclohexane confirm the results of [1]. For SNH solutions, the specific rotatory power $[\alpha]_{589}$ is -3, while for SNO* $[\alpha]_{436}$ is $+28$. For SNO* solutions, two positive dichroic bands are observed at 240 nm ($\Delta\varepsilon = +1$) and 420 nm ($\Delta\varepsilon = +0{\cdot}3$) corresponding to UV absorptions at $\lambda_{max} = 245$ nm ($\varepsilon = 1900$) and $\lambda_{max} = 450$ nm ($\varepsilon = 14$), respectively. The latter absorption is assigned to the forbidden $n \rightarrow \pi^*$ transition involving the single nitroxide electron and is responsible for the slight orange colour of the samples.

3.2. *Sol phases*

Data collection is made during the induction delay of the kinetic steroid aggregation process at room temperature. First, for dilute transparent gels, the optical rotation values are comparable to that of dilute solutions. Secondly, the SNH sols do not display any significative dichroic signal as expected since no UV absorption occurs in the wavelength range recorded. For SNO* ($C = 1{\cdot}6 \times 10^{-2}$ M), two dichroic bands ($\Delta\varepsilon_{250} = +1{\cdot}5$ and $\Delta\varepsilon_{450} = +0{\cdot}37$) are observed similar to that for the dilute non-gelling solutions (see the table).

Indicative values for dichroic absorption during the SNO* sol–gel transition.

	(1)	(2)	(3)	(4)	(5)	(6)	(7)	(8)	(9)
λ nm	ε	←			$\Delta\varepsilon$ or $\lvert\Delta\varepsilon\rvert$				→
450	13	+0·26	+0·35	+0·4	+0·45	+0·4	+0·4	+0·5	+0·45
245	1900	+1	+1·5	6·0	12	8	15	25	33

(1) and (2), dilute non-gelling cyclohexane solutions [1] $C_0 = 7{\cdot}4 \times 10^{-4}$ M; (3), sol phase $C_0 = 1{\cdot}6 \times 10^{-2}$ M; (4), gel phase $H = 0$ T, $d = 0{\cdot}01$ dm, $C_0 = 1{\cdot}6 \times 10^{-2}$ M; (5), gel phase $H = 7$ T, $d = 0{\cdot}01$ dm, $C_0 = 1{\cdot}6 \times 10^{-2}$ M; (6), gel phase $d = 0{\cdot}01$ dm, $C_0 = 2{\cdot}1 \times 10^{-2}$ M; (7), gel phase $d = 0{\cdot}002$ dm, $C_0 = 2{\cdot}1 \times 10^{-2}$ M; (8), gel phase $d = 0{\cdot}001$ dm, $C_0 = 4{\cdot}0 \times 10^{-2}$ M; (9), gel phase $d = 0{\cdot}002$ dm, $C_0 = 8{\cdot}0 \times 10^{-2}$ M. We note that the concentration, the width of the cell and the use of a strong magnetic field are efficient orientating parameters.

3.3. *Gel phases*

3.3.1. *Birefringence measurements*

A transparent dilute ($C_0 = 2{\cdot}7 \times 10^{-2}$ M) SNH gel (or SNO* $C_0 = 1{\cdot}2 \times 10^{-2}$ M) does not exhibit a significative and reproducible variation of the rotatory power during the sol → gel transition in the wavelength range studied. In contrast, for slightly turbid gels (more concentrated or a lower temperature) larger values

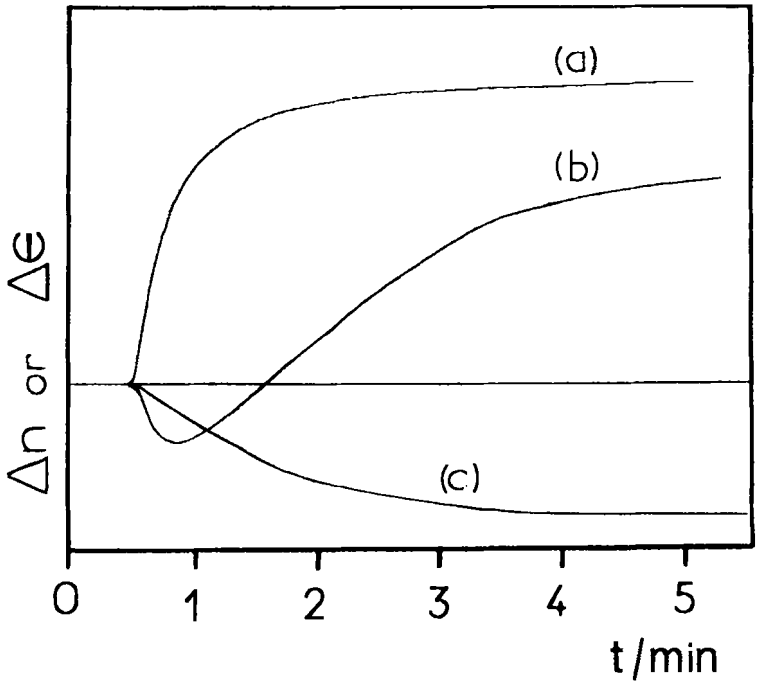

Figure 2. Kinetic record for the sol → gel transition. Birefringence example: SNH solution $C_0 = 2{\cdot}5 \times 10^{-2}$ M, cell width $d = 0{\cdot}01$ dm, $|\Delta(\Delta n(t))|\rightarrow \approx 30 \times 10^{-6}$. For dichroism values see the table. (*a*), (*b*), (*c*) for three different experiments: (*a*) dominating oriented domain, (*b*) polydomains, (*c*) domain(s) grown in an orthogonal direction compared to (*a*).

($|[\alpha]_{436}| \approx 250$) are recorded but these are probably not associated with an intrinsic property of the steroid aggregate but rather with a collective interparticular contribution from the colloidal dispersion (linear effects).

The fibre orientation in these systems can be accidental (anchoring on the surfaces of the cell and by excluded volume effects [4]) or induced by a strong magnetic field. The growth of oriented microdomains is studied by recording the kinetic variation of the birefringence $\Delta n(t)$ without and with a magnetic field during the sol → gel transition. Figure 2 shows the various profiles which can be observed, from a regular sigmoid to more complex curves (see the figure caption for numerical values). The laser beam experiences the average orientation of one or several growing micronic or submicronic gel domains. $\Delta n(t)$ reflects the dispersion of the orientation director and the spatial extension of the growing volumic domains crossed by the laser beam. In the absence of a strong external magnetic field, the resultant orientation of the mosaic of microdomains can be reversed by the germination and growth of a new dominating oriented region. This explains the particular shape of the kinetic curve 7*b* (see figure 2).

With a strong magnetic field the ordering can be very significant [6] when oriented/collapsed solid bundles of fibres phase separate from the sample. Reproducibility is poor because the development of the oriented growth precursors is very sensitive to all of the usual parameters of the germination processes in supersaturated systems. The critical kinetic increase of the length of fibres during the steroid aggregation [6] quickly prevents any aggregate reorientation. At least, no more sign inversion in the

slope $d(\Delta n(t))/dt$ (or $d(\Delta\varepsilon(t))/dt$ in the case of similar dichroic experiments at a fixed wavelength) is observed when the orientation process is suspected to be successful. The distribution of the directors describing the preferred orientation of each constitutive microdomain of the sample has become significantly narrower or the size of one of these domains has become dominating.

3.3.2. *Dichroism measurements*

Random fibrillar growth: sol → gel transition without a magnetic field. Figures 3, 4 and 5 show the dichroic spectra for SNO* gel samples. The spectra show two regions: 200/300 nm with very variable intense profiles (these can be present in SNH as well, which was unexpected) and the 450 nm wavelength region which always exhibits a positive dichroic absorption almost insensitive to the cell position (see figure 5) with respect to the light beam (absent for SNH). This latter dichroism band could be used as an internal probe of the radical concentration in the gel sample. The variations of the dichroic intensities with the angle α of the cell in the orthogonal plane with respect to the polarization direction of light can be used as an indicator of the orientational order in the gel sample. For a SNO* sample ($C_0 = 2{\cdot}1 \times 10^{-2}$ M) in a 0·01 dm cell, $R_{250} \to -1$ since ellipticities $[\theta]$ between + 20 000 ($\Delta\varepsilon_{250} = +6{\cdot}1$) and − 25 000 ($\Delta\varepsilon = -7{\cdot}6$) can be measured at 250 nm. At 450 nm the dichroic transition has a very moderate amplitude variation ($R_{450} = 1{\cdot}6$, $+0{\cdot}31 < \Delta\varepsilon < +0{\cdot}5$). The intensity of the 250 nm linear dichroic absorption is sensitive to the cell width: $|\Delta\varepsilon_{250}| \approx 8$ if $d = 0{\cdot}01$ dm and *c.* 15 if $d = 0{\cdot}002$ dm for a $C_0 = 2{\cdot}1 \times 10^{-2}$ M SNO* gel (see also figures 3 and 4). This indicates that the cell itself acts as an orientating device for fibres orientation.

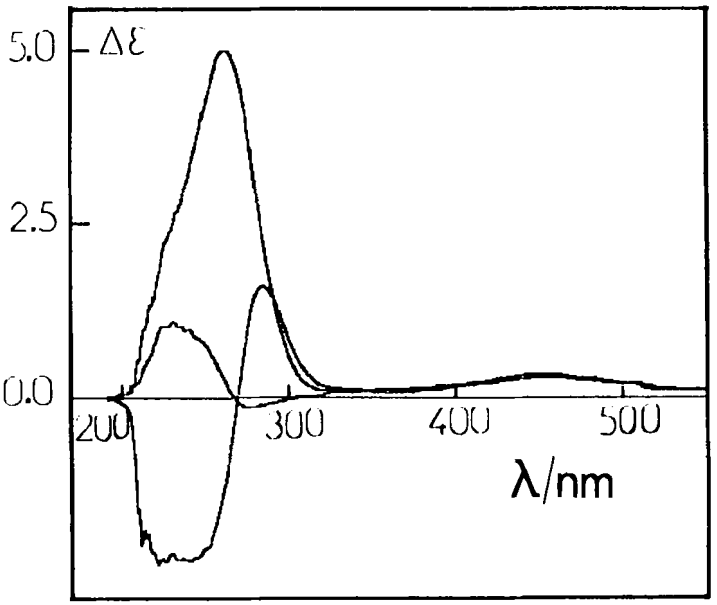

Figure 3. Dichroism spectra: SNO*, random gel growth, cell width $d = 0{\cdot}01$ dm. $C_0 = 2{\cdot}0 \times 10^{-2}$ M. The three curves are for various orthogonal positions of the cell with respect to the polarized light.

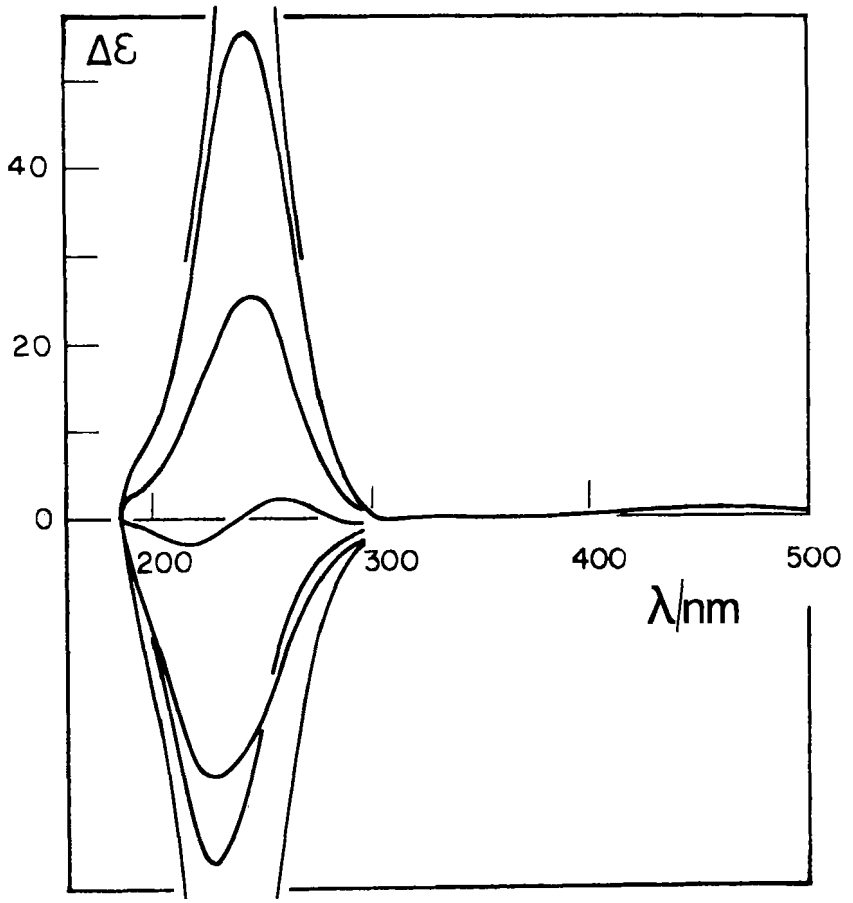

Figure 4. Dichroism spectra: SNO*, random gel growth, cell width $d = 0{\cdot}001$ dm. $C_0 = 8{\cdot}0 \times 10^{-2}$ M. Different curves for various orthogonal positions of the cell with respect to the polarized light. Main absorption $\lambda_{max} = 239$ nm. Note that the weak dichroic absorption at 450 nm is nearly insensitive to the cell position. The dichroic band in the 200–300 nm range exhibits extreme positive and negative values indicating the high orientational order of the steroid gel.

Tests to eliminate the linear component have beem made but it was impossible to eliminate it completely because the microdomains are randomly scattered within the volume crossed by the UV radiation. Nevertheless, the linear dichroism appears to be the major contribution in the 200–300 nm dichroic absorption and correlated with the UV absorption at $\lambda_{max} = 245$ nm as noted in the table. The existence of circular as well as selective reflection components cannot be excluded and have to be searched for in oriented bidimensional gel phases (films).

Figures 6 and 7 show the dichroic signals for the SNH gels. The dichroic signal which appears from the flat spectrum ($\Delta\varepsilon_{250} < 0{\cdot}003$) of the sol phase in the 200–300 nm region ($|\Delta\varepsilon| < 4$) correspond to UV absorption which cannot be neglected at this reaction rate (for instance, for $C_0 = 4{\cdot}1 \times 10^{-2}$ M and $\lambda = 350$ nm, $A = 0{\cdot}06$ at $t = 1$ min; $A = 0{\cdot}126$ at $t = 15$ min). The dichroic absorption occurs at shorter wavelengths and is mainly a linear contribution because of its sensitivity to the cell

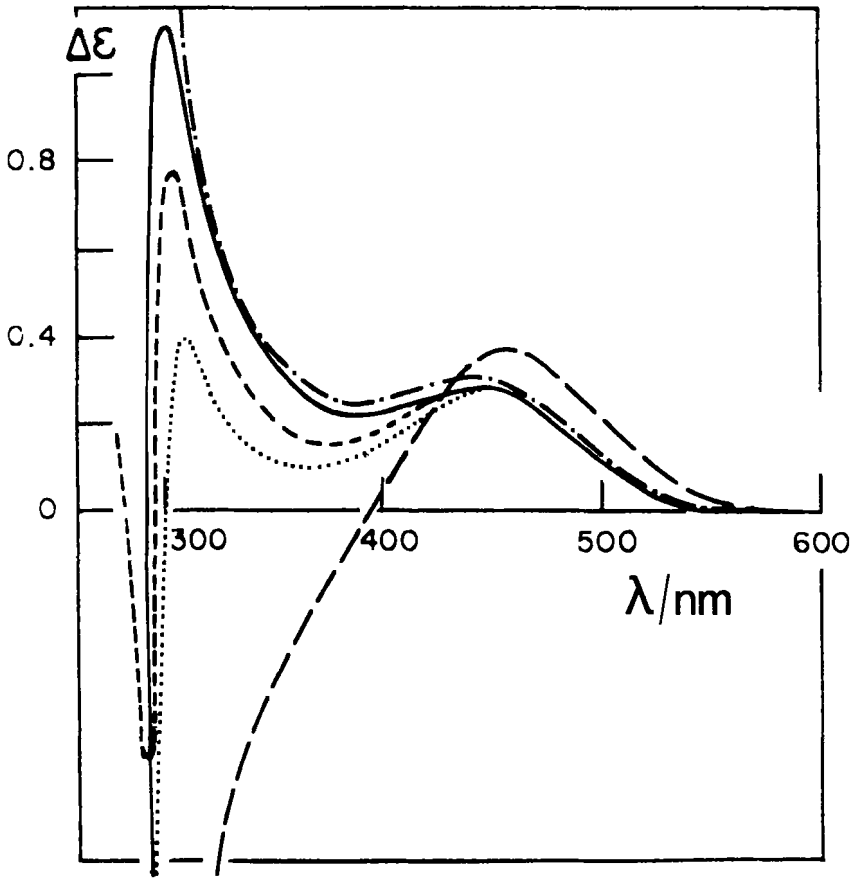

Figure 5. Dichroism spectra: SNO* gel sample, random gel growth, cell width $d = 0{\cdot}1$ dm. $C_0 = 2{\cdot}0 \times 10^{-2}$ M. Details of the 300–500 nm range. Different curves for various orthogonal positions of the cell with respect to the polarized light.

orientation (see figures 6 and 7). Again the signal is a function of the sample width ($|\Delta\varepsilon_{250}| \approx 0{\cdot}2$ for $d = 0{\cdot}1$ dm and *c.* 3 for $d = 0{\cdot}002$ dm). We note that it is possible to obtain a gel phase which does not exhibit any significative dichroic absorption for a given cell orientation: this is an indication that the signal is mainly a linear contribution.

Oriented fibrillar growth: sol → gel transition in a strong magnetic field. Again, the optical method (birefringence and dichroism) can be used to evaluate the fibre orientation in the samples. The dichroic kinetic curves $[\theta]_{(t)}$ (see figure 2) no longer exhibit sign inversion at a fixed wavelength and the sensitivity to the cell position in the beam is extreme ($R_{250} \to -1$). Figure 6 illustrates the magnetic orientation obtained for SNH samples in a cell 0·1 dm thick. The kinetic record of $[\theta]_{(t)}$ during the sol–gel transition at a fixed wavelength ($\lambda = 250$ nm) can be used to follow the reaction rate and the orientation order. Figure 2 (*a*) shows an example of such a single or dominant oriented growing domain.

As for birefringence measurements, we conclude that the sample is much more homogeneous (less microdomains of different orientation with respect to the orientating magnetic field and analysing electric field). Even though we cannot exclude the

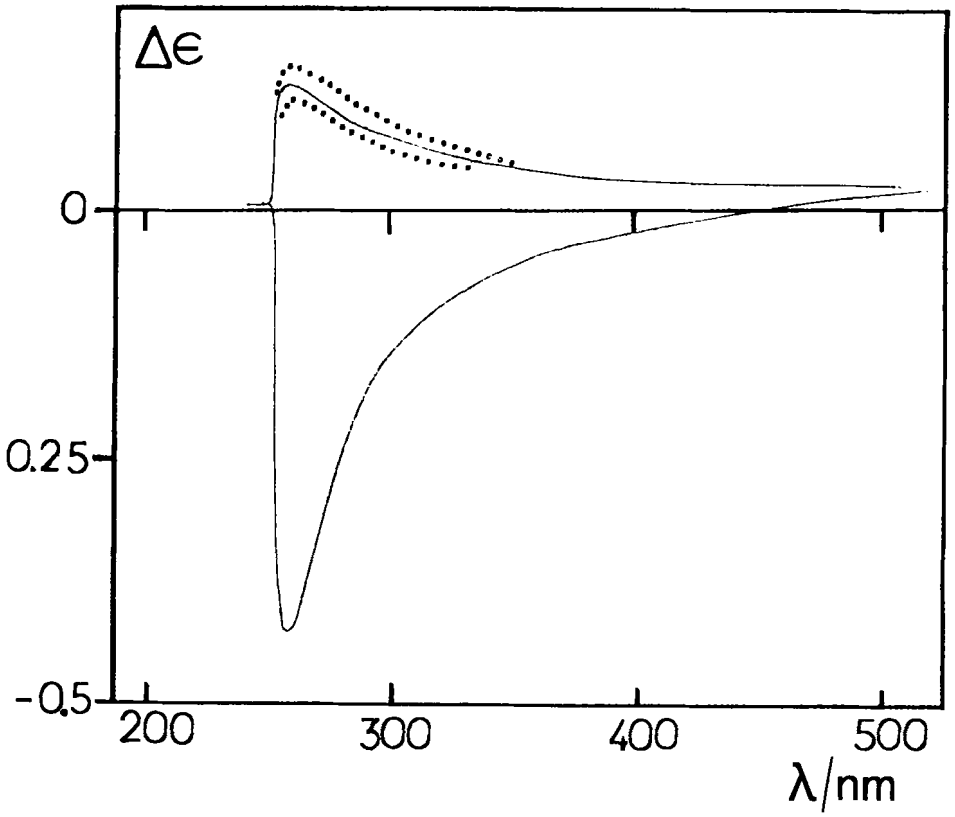

Figure 6. Dichroism spectra: SNH gel sample, cell width $d = 0{\cdot}1$ dm, $C_0 = 3{\cdot}0 \times 10^{-2}$ M. Plain curves: gel grown in a magnetic field, gel unperfectly oriented, two orthogonal cell positions; dashed curves: random gel growth.

existence of a circular component, this is not the major contribution in the dichroic spectra of such systems.

4. Discussion and conclusion

These experiments have emphasized that optical determinations on such phases are delicate. This is inherent to the special status of the gel phases in physical chemistry. Both properties of a liquid (viscosity, transparency etc....) and of a solid (elasticity) are involved, the concentration range itself could be likened to that of entangled semi-dilute regime of polymers in solution [12], typical dimensions are that of colloids which interact strongly with light: consequently the related optical techniques are very sensitive to any structural change in the submicronic range of these interconnected aggregates of the gel network. The situation is considerably simpler for dilute solutions of finite micelles where the techniques can be used for the determination of structural configurations of the aggregates [13, 14].

The optical rotatory power data suggest that the steroid fibres made up with fibrils could develop chirality mainly in the junction zones. Previous electron microscopy studies [3] with a freeze-fracture procedure have shown such helical entwinning of steroid fibres and fibrils within the junction zones of the gel network. Once the concentration of these zones is high enough, the optical rotatory power is strikingly

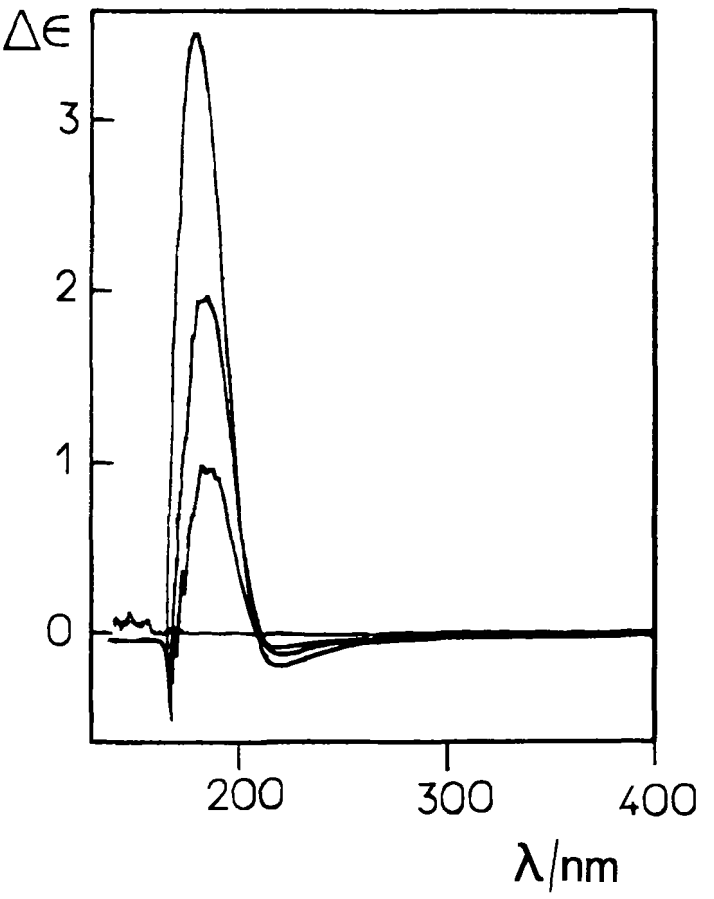

Figure 7. Dichroism spectra: SNH gel sample, random gel growth, cell width $d = 0{\cdot}002$ dm, $C_0 = 3{\cdot}0 \times 10^{-2}$ M. Main absorption $\lambda_{max} = 180$ nm. Different curves for various orthogonal positions of the cell with respect to the polarized light.

increased, as well the light scattering and the heterogeneity of the now more or less turbid sample. Complementary measurements have to be performed in an extended wavelength range (200–400 nm) to determine the complete optical rotatory dispersion (ORD) curve. We note that the present experiments have been performed in a region where there is a Cotton effect due to UV absorption from the nitroxide group in the SNO* derivative. By contrast, in numerous polysacharride biopolymers [15] (gelatin, carrageenans, agarose) where the basic fibres and fibrils are chiral, optical rotation can be used as an accurate kinetic titration method during the renaturation process generating the gel network.

Dichroism detected in the SNO* gel samples is mainly due to linear contributions in the 200–300 nm region but the existence of a circular contribution cannot be estimated from this kind of volumic samples. The 400–500 nm range exhibits the dichroic absorption typical of the nitroxide chromophoric group: it is mainly a circular contribution and its intensity, comparable to that of solutions, indicates that the chiral nitroxide chromophoric group is not a probe in this wavelength region of a supramolecular chirality.

The amplitude of the linear signal is not only dependent upon the steroid concentration but is also sensitive to the overall history of the sample. Temperature and the use of external orientating forces (magnetic fields, width of the cell) are among the operative parameters. The shape of the dichroism signal can be complex and recalls in some ways that of DNA and some other polynucleotide systems [15, 16] (positive and negative components in the 200–300 nm region as predicted for helical arrangement of chromophores [17]). We note that previous electron microscopy studies [3] have shown some helical and super twisted structures. This super twisting occurs as a relaxation process of stressed chiral fibres for which the extremities which are the nodes of the gel network are approached (for instance by solvent evaporation). These superstructures are comparable to those in DNA [18]. For oriented DNA films, it is shown that the spectra obtained, which also show a very high angular dependence as the film is rotated about the axis of the beam, can be interpreted as the sum of two components, the actual circular dichroism term plus a linear dichroism component [11]. Despite their different chemical constitution, DNA and steroids exhibit some interestingly comparable properties. We note that for some aromatic cholesteryl derivatives which contain a comparable steroid unit, it has also been concluded that the molecules are helically stacked [2].

We have shown that both linear birefringence and dichroism ($\lambda = 250$ nm) can be used to reveal the orientational order in the microdomains of the volume crossed by the light beam. Kinetic records can be conveniently used to follow the orientational order in a sol–gel transition experiment. Further experiments are in progress on oriented films to study the linear contribution with the help of the so-called Hermans orientation function [19] or orientational order parameter

$$f = \frac{(3\langle\cos^2\theta\rangle - 1)}{2}. \tag{7}$$

Here θ is the angle between the chain axis and the reference direction for the birefringence while for the dichroism the angle between the transition moment of the absorbing group with respect to the chain has to be taken into account. As an example, optical properties have already been used to characterize the orientation of collagen fibres [20], various polymers [21] or dye aggregates in a flow gradient [22].

By contrast, organogels of a 12-hydroxystearic compound which contains an asymmetric carbon (C_{12}) responsible of the growth of helical structures, an enantimorphic relation exists between the molecular chirality and that of the supramolecular fibrillar aggregates. A selective reflection mechanism has been proposed [23, 24] to explain the dichroic spectra.

As a conclusion, steroid gels appear to behave differently compared to the two reference physical gels: polysaccharide aqueous gels and 12-hydroxystearic organogels. This difference arises from the gelation mechanism itself (molecular symmetry and stericity) and the optical methods developed here constitute a promising way of investigation. Extra circular birefringence and dichroism can only be analysed fully with oriented bidimensional gels, the preparation of which is under progress.

The author is grateful to Drs R. Ramasseul and F. Volino, for their interesting discussions concerning the topic. Dr. J. Torbet is specially thanked for his help in optical birefringence measurements. Mr. E. Tasset is thanked for his technical participation to the work.

References

[1] MARTIN-BORRET, O., RAMASSEUL, R., and RASSAT, R., 1979, *Bull. Soc. Chim. Fr.*, p. 401.
[2] LIN, Y., KACHAR, B., and WEISS, R. G., 1989, *J. Am. chem. Soc.*, p. 5542.
[3] TERECH, P., and WADE, R. H., 1988, *J. Colloid Interface Sci.*, **125**, 542 and references cited therein.
[4] TERECH, P., 1989, *J. Phys., Paris*, **50**, 1967 and references cited therein.
[5] TERECH, P., 1989, *Molec. Crystals liq. Crystals*, **166**, 29.
[6] TERECH, P., 1989, *Prog. Colloid Polym Sci.*, **79**, 81.
[7] MARET, G., and DRANSFELD, K., 1977, *Physica* B, **86/88**, 1077.
[8] HATANO, M., 1986, *Advances in Polymer Science*, Vol. 77 (Springer), p. 1.
[9] LEVIN, A. I., and TINOCO, I., 1977, *J. chem. Phys.*, **66**, 3491.
[10] SAEVA, F. D., and WYSOCKI, J. J., 1977, *J. Am. chem. Soc.*, **93**, 5928.
[11] TUNIS-SCHNEIDER, M. J., and MAESTRE, M. F., 1970, *J. molec. Biol.*, **52**, 521.
[12] SCHAEFER, D. W., 1984, *Polymer*, **25**, 387.
[13] KUNITAKE, T., NAKASHIMA, N., SHIMOMURA, M., OKAHATA, Y., KANO, K., and OGAWA, T., 1980, *J. Am. chem. Soc.*, **102**, 6644.
[14] D'ALAGNI, M., FORCELLESE, M. L., and GIGLIO, E., 1985, *Colloid Polymer Sci.*, **263**, 160.
[15] CLARK, A. H., and ROSS-MURPHY, S. B., 1987, *Advances in Polymer Science*, Vol. 83 (Springer-Verlag), p. 57 and references cited therein.
[16] WARSHAW, M. M., and NOE, R., 1972, *Biopolymers*, **11**, 1269.
[17] MOFFITT, W., 1956, *J. chem. Phys.*, **25**, 467.
[18] SAENGER, W., 1984, *Principles of Nucleic Acid Structure* (Springer-Verlag).
[19] HERMANS, P. H., 1946, *Contributions to the Physics of Cellulose Fibres* (Elsevier).
[20] CHANG, E. P., and CHIEN, J. C. W., 1973, *Biopolymers*, **12**, 2751.
[21] SIESLER, H. W., 1984, *Advances in Polymer Science*, Vol. 65 (Springer-Verlag), p. 1.
[22] NORDEN, B., 1977, *J. phys. Chem.*, **81**, 151.
[23] TACHIBANA, T., MORI, T., and HORI, K., 1980, *Bull. chem. Soc. Japan*, **53**, 171.
[24] SAKAMOTO, K., YOSHIDA, R., HATANO, M., and TACHIBANA, T., 1978, *J. Am. chem. Soc.*, **100**, 6898.